

4-Substituted Trinems as Broad Spectrum β -Lactamase Inhibitors: Structure-Based Design, Synthesis, and Biological Activity[†]

Ivan Plantan,[†] Lovro Selič,[†] Tomaž Mesar,[†] Petra Štefanič Anderluh,[†] Marko Oblak,[†] Andrej Preželj,[†] Lars Hesse,[‡] Miha Andrejašič,[§] Mateja Vilar,[†] Dušan Turk,[§] Andrej Kocijan,[†] Tadeja Prevec,[†] Gregor Vilfan,[†] Darko Kocjan,[†] Anton Čopar,[†] Uroš Urleb,[†] and Tom Solmajer^{*,†,§,⊥}

Drug Discovery, Lek Pharmaceuticals d.d., Verovskova 57, SI-1526 Ljubljana, Slovenia, National Institute of Chemistry, POB 660, Hajdrihova 19, 1001 Ljubljana, Slovenia, Antibiotic Research Institute, Sandoz, A-1235 Wien, Austria, and Department of Biochemistry and Molecular Biology, Jožef Stefan Institute, Jamova 39, SI-1000 Ljubljana, Slovenia

Received March 21, 2007

A wide variety of pathogens have acquired antimicrobial resistance as an inevitable evolutionary response to the extensive use of antibacterial agents. In particular, one of the most widely used antibiotic structural classes is the β -lactams, in which the most common and the most efficient mechanism of bacterial resistance is the synthesis of β -lactamases. Class C β -lactamase enzymes are primarily cephalosporinases, mostly chromosomally encoded, and are inducible by exposure to some β -lactam agents and resistant to inhibition by marketed β -lactamase inhibitors. In an ongoing effort to alleviate this problem a series of novel 4-substituted trinems was designed and synthesized. Significant *in vitro* inhibitory activity was measured against the bacterial β -lactamases of class C and additionally against class A. The lead compound LK-157 was shown to be a potent mechanism-based inactivator. Acylation of the active site Ser 64 of the class C enzyme β -lactamase was observed in the solved crystal structures of two inhibitors complexes to AmpC enzyme from *E. cloacae*. Structure–activity relationships in the series reveal the importance of the trinem scaffold for inhibitory activity and the interesting potential of the series for further development.

Introduction

Infectious diseases are among the leading causes of mortality. A wide variety of pathogens have acquired antimicrobial resistance as an inevitable evolutionary response to the extensive use of antibacterial agents. Surveillance data indicate that resistance has arisen to all established antibacterial classes, including new agents with novel mechanisms of action, and has spread between and within bacterial populations with great efficiency. The dramatic increase in antibacterial resistance in both community and hospital settings has resulted in therapeutic failures with increased morbidity, mortality, and healthcare costs.^{1–3}

Although bacteria have developed several strategies for escaping the lethal action of β -lactam antibiotics, the most common and often the most efficient mechanism is the synthesis of β -lactamases. These enzymes, which are usually secreted into the external medium by Gram-positive species and into the periplasm by their Gram-negative counterparts, catalyze the irreversible hydrolysis of the amide bond of the β -lactam ring, yielding biologically inactive products.^{4,5}

On the basis of amino acid sequence similarities, β -lactamases have been broadly grouped into four molecular classes, A, B, C, and D. The diversity of the β -lactamases is a most critical aspect of antimicrobial therapy. The β -lactamase superfamily currently has more than 450 members, many of which differ only by a single amino acid (www.lahey.org).

Enzymes of classes A, C, and D are active site serine β -lactamases, whereas class B enzymes are metallo- β -lactamases that contain a zinc atom at the active site. Class A enzymes are primarily penicillinases, mostly plasmid-mediated, usually constitutively expressed and susceptible to inhibition by the clinically available β -lactamase inhibitors. Class C enzymes, in contrast, are primarily cephalosporinases, mostly chromosomally encoded, inducible by exposure to some β -lactam agents, and resistant to inhibition by β -lactamase inhibitors.^{6,7}

Much effort has been devoted to the synthesis of β -lactam agents which would bypass this defense mechanism, but the changing epidemiology of β -lactamases has rendered these novel agents inactive following their introduction to clinical use. A highly effective approach for tackling β -lactamase-mediated resistance to β -lactams is the use of β -lactam agent/ β -lactamase–inhibitor combinations, where the latter potentiates the action of the former by protecting it from enzymatic hydrolysis.⁸ Commercially available inhibitors potassium clavulanate, sulbactam, and tazobactam, inhibit most class A and some class D β -lactamases, but activity against class C types is poor. Detailed knowledge of the binding mode of β -lactamase inhibitors used in the clinic should facilitate the design of second generation β -lactamase inhibitors that possess broad-spectrum activity against clinically relevant producers of class A, class D, and class C enzymes.⁹ The efficacy and safety of β -lactams as a class has provided powerful motivation for the development of novel molecules which would address the unmet medical needs posed by bacterial resistance. The alkylidene penems and 2 β -substituted penam sulfones, oxapenems, cephalosporin-derived compounds, cyclic acyl phosphonates, and non- β -lactam compounds are currently under investigation as potential β -lactamase inhibitors, but their clinical applications are not yet available.^{10–14}

[†] This paper is dedicated to the late Professor J.-M. Ghuysen (University of Liege) in honor of his pioneering work in the field.

* To whom correspondence should be addressed. Phone: +386-1-4760 277; Fax: +386-1-4760-300; E-mail: tom.solmajer@ki.si; tom.solmajer@sandoz.com.

[†] Lek Pharmaceuticals d.d.

[‡] National Institute of Chemistry.

[§] Sandoz.

[⊥] Jožef Stefan Institute.

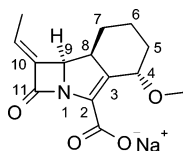


Figure 1. Chemical structure of lead compound (8*S*,9*R*)-10(*E*)-ethylidene-4(*S*)-methoxy-11-oxoazatricyclo[7.2.0.0.3.8]undec-2-enecarboxylate, with trinem numbering included.

Recently, following a rational structure-based drug design approach, novel tricyclic carbapenem (trinem^a) compounds with tetrahydro-2*H*-thiopyran and/or adjacent fused cyclohexane rings were synthesized by our research group (Figure 1).^{15,16} The fusion of the hydrophobic cyclohexane or 6-thia ring onto the carbapenem moiety, which was hypothesized to arrest the deacylation step of the tetrahedral acyl-enzyme intermediate¹⁵ by blocking the access of water, was found to augment inhibitory activity toward class C and class A β -lactamases (unpublished work from this laboratory). However, by introducing the 4-methoxy substituent^{16,17} to the trinem scaffold, the inhibitory activity was enhanced by 2 orders of magnitude *in vitro* to both enzymes AmpC β -lactamase (class C) and TEM 1 β -lactamase (class A) from *E. coli*. On the basis of these preliminary findings, we did not pursue the development of the unsubstituted trinem compounds any further.

In the present paper we report on the design, improved synthesis procedure, and inhibitory activity of novel 4-substituted trinems as broad-spectrum β -lactamase inhibitors of both class A and class C enzymes. In addition, the solved crystal structure of our lead compound **11a** (Figure 2), selected from a series of ethylidene derivatives of tricyclic carbapenems in complex with AmpC β -lactamase from *Enterobacter cloacae*, offers a possible explanation for its *in vitro* efficacy, which was determined to be superior to clinically available β -lactamase inhibitors. In addition, the solved crystal structure of the 4-butyloxy derivative offers a possible explanation to the structure–activity relationship of 4-substituted derivatives with variable lipophilicity.

Chemistry. The designed 4-alkoxy-10-ethylidene trinem analogues were prepared employing previously described synthetic procedures¹⁸ for trinem scaffold synthesis, followed by ethylidene moiety formation and allyl ester deprotection. These procedures were significantly optimized to give intermediates with considerably higher yields.

Two different synthetic procedures were used (Scheme 1) to prepare the key intermediates, (3*R*)-[(1*R*)-(tert-butyl)dimethylsilyloxy]-ethyl]-4(*R*)-((1*S*/*R*)-(3*R*/*S*)-alkoxy-2-oxo-cyclohexyl)-azetidin-2-ones (**4a–h**). According to synthetic route I, the starting 2-alkoxycyclohexanones **2c,d** were synthesized, using known synthetic procedures, from cyclohexene oxide,¹⁹ except for the 2-methoxy- and 2-ethoxycyclohexanones (**2a, 2b**) which were commercially available. Coupling of the corresponding 2-alkoxycyclohexanones **2a–d** with ((3*R*,4*R*)-3-((1*R*)-1-[[tert-butyl(dimethyl)silyl]oxy]ethyl)-4-acetoxy-2-azetidinone **3**, in the presence of SnCl₄ as a Lewis acid, afforded the mixtures of (1'*R*,3'*S*) and (1'*S*, 3'*R*) diastereomers **4a–f**, which were separated by column chromatography or by crystallization.²⁰ The 2-fluoroethoxy and 2-cyanoethoxy intermediates **4g** and **4h** were prepared *via* synthetic route II, which included the stereoselective opening of epoxide²¹ **5** with 2-fluoroethanol and 3-hydrox-

ypionitrile, respectively. Since the yields of the previously described methods did not render realization of the six synthetic steps for the preparation of 2-fluoroethoxy and 2-cyanoethoxy final compounds **11g,h** possible, it was necessary to prepare adequate quantities of 2'-alkoxy-1-hydroxycyclohexylazetidinones **6g,h**.²²

In view of these complexities the ultrasonically aided opening of epoxide **5**, with triflate catalysts, was studied.²³ According to those findings, **6g** was prepared from 2-fluoroethanol with a 52% yield, and **6h** from 3-hydroxypropionitrile with a 55% yield. Subsequent Swern oxidation²⁴ of **6g,h** yielded **4g,h**.

The pure diastereomers **4a–h** (at least 96% de) obtained by synthetic routes I and II were further acylated with allyl oxallyl chloride and cyclized with triethyl phosphite in refluxing xylene in the presence of hydroquinone to give the trinem intermediates **8a–h**.²⁵ Subsequent deprotection of the *tert*-butyldimethylsilyl group by tetrabutylammonium fluoride provided intermediates **9a–h**.²⁶ In order to prepare the designed ethylidene moiety on the trinem scaffold, various synthetic approaches were studied, among which only water elimination under the conditions of the Mitsunobu reaction²⁷ enabled the preparation of isomers **10a–h** possessing the exclusively *E* configuration of the ethylidene group.²⁸ The byproducts of the Mitsunobu reaction, triphenylphosphine oxide and diethyl hydrazine-1,2-dicarboxylate, were removed by selective precipitation with diethyl ether and the crude products further purified with column chromatography.

In the last step, allyl group deprotection with sodium 6-ethylhexanoate, Pd[(PPh)₃]₄ and PPh₃ in tetrahydrofuran afforded target compounds **11a–h**.²⁹ In general, the final compounds precipitated from the reaction mixture spontaneously or after addition of diethyl ether or petroleum ether; otherwise extraction to water medium and subsequent lyophilization was necessary.

Results and Discussion

Determination of the Acyl-enzyme Complex Structure.

Several structures of β -lactamases from both classes A and C have been available for some time now.^{30–41} Their use for the design, using computer-assisted molecular modeling, of novel molecules is necessitated and based on the knowledge of the complex enzyme–inhibitor structure.

However, the principal reason for a possible uncertainty in this procedure is that the reactions of the inhibitors with β -lactamases frequently involve branched pathways with a variety of putative intermediates. A manifested example of such a process was the solved structure of the complex clavulanate- β -lactamase TEM-1 from *E. coli*, in which an unexpected breakup of the clavulanate ligand was observed.⁴² Thus, we deemed it necessary to substantiate our mechanistic hypothesis and attempt to explain the inhibitory activity of the trinem series toward β -lactamases of class C by solving the structure of the complex AmpC β -lactamase from *Enterobacter cloacae* with two compounds from the trinem series. **11a** was chosen due to its inhibitory potency in the nanomolar range toward both class A and class C β -lactamases.¹⁷ A second structure of the complex AmpC β -lactamase with 4-butyloxy trinem derivative (vide infra) was solved to provide clues to structure–activity relationship of inhibitors series designed to optimize ADME properties of the lead compound **11a**.

Interactions of the Acyl-enzyme Intermediate in the AmpC Binding Site. The crystal structure of the complex revealed the presence of inhibitor **11a** covalently linked to the O γ atom of the Ser 64 side chain in the AmpC active site (Figure

^a Abbreviations: trinem, tricyclic carbapenem; EDIPA, *N,N*-diisopropylethylamine; TBAF, tetra-*n*-butylammonium fluoride; THF, tetrahydrofuran; DEAD, diethyl azodicarboxylate; PEG, polyethylene glycol; PMSF, phenylmethanesulfonyl fluoride.

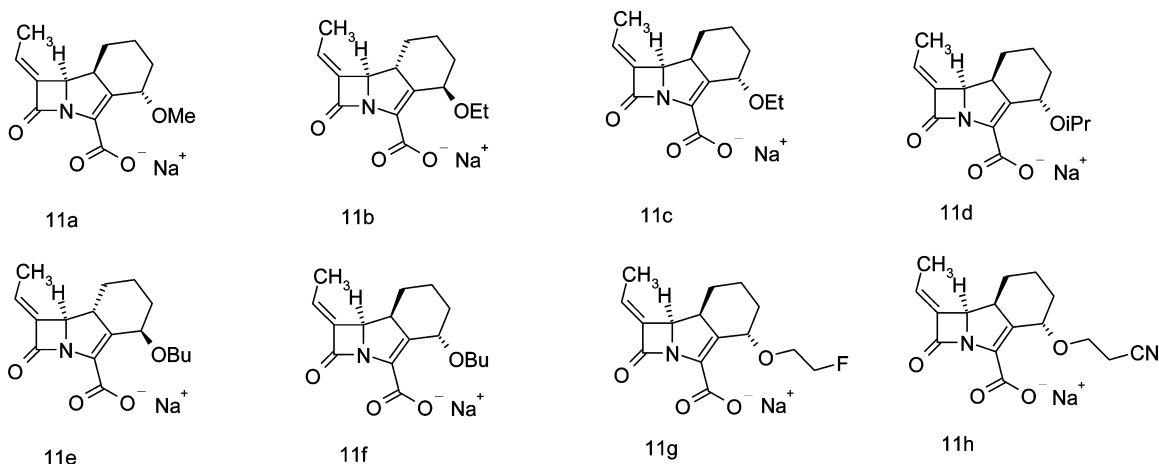
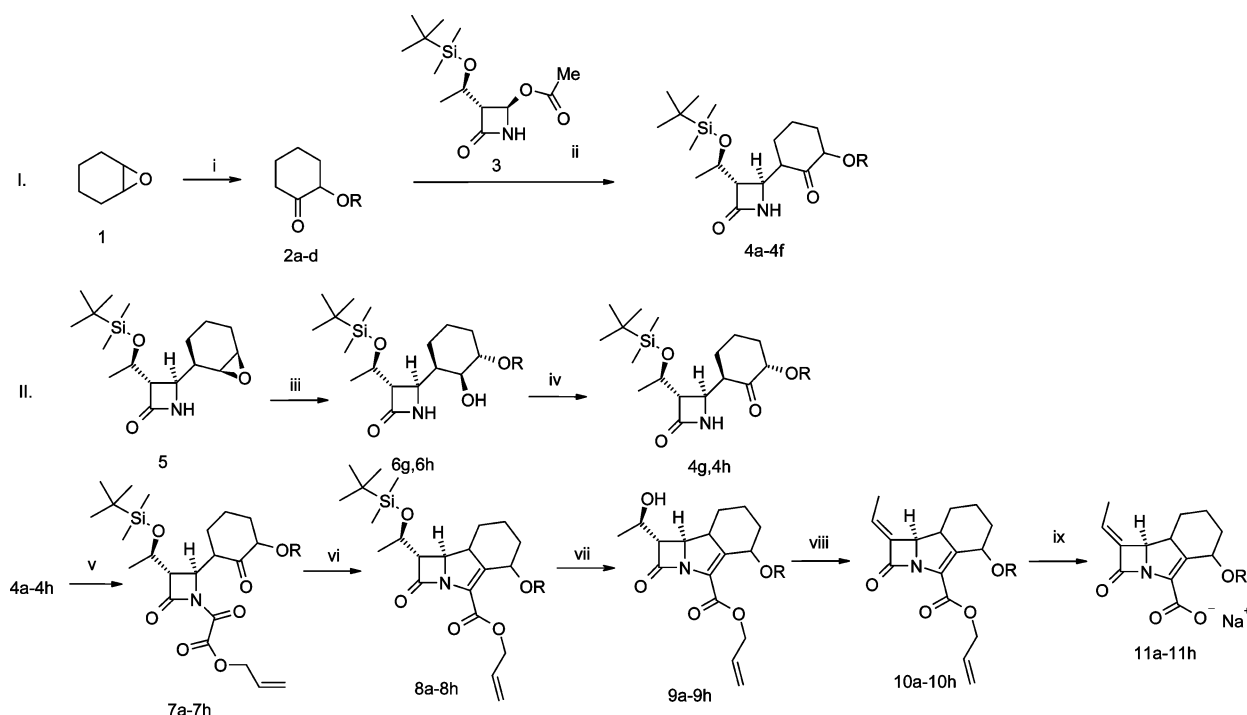


Figure 2. Structures of the synthesized compounds illustrating stereoisomerism at substituents 4 and 8.

Scheme 1^a



^a Reagents and conditions: (i) 1. ROH, FeCl₃, r.t.; 2. Pyridinium chlorochromate, CH₂Cl₂, r.t.; (ii) 1. SnCl₄, CH₂Cl₂, **3**, 0 °C, 2. EDIPA, 0 °C; (iii) for **6g**: FCH₂CH₂OH, Yb(OTf)₃, ultrasound; for **6h**: NCCH₂CH₂OH, Sn(OTf)₂, ultrasound; (iv) 1. (COCl)₂, DMSO, CH₂Cl₂, 2. Et₃N; (v) for **7a–f**: allyl oxallyl chloride, Et₃N, CH₂Cl₂, 0 °C; for **7g**, **7h**: allyl oxallyl chloride, Et₃N, K₂CO₃, CH₂Cl₂, 0 °C; (vi) (EtO)₃P, hydroquinone, xylene, reflux; (vii) 1 M TBAF, AcOH, THF, r.t.; (viii) PPh₃, DEAD, CH₂Cl₂, 0 °C; (ix) PPh₃, Pd[(PPh₃)₃]₄, NaOH, THF, r.t.

3). The β -lactam carbonyl oxygen of **11a** is oriented in the oxyanion hole, forming two hydrogen bonds with the backbone amide groups of Ser 64 (2.9 Å) and Ser 318 (3.0 Å). In turn, the acyl intermediate appears to be well positioned in the active site, forming numerous hydrophobic interactions with the nonpolar side chains of residues Leu 119 and Leu 293.

Surprisingly, the carboxylic group of **11a** is directed out of the active site and has no direct interactions with the enzyme. In the structure of the noncovalent Michaelis complex⁴³ of a cephem sulfone which is a step in the mechanism prior to the acyl-enzyme formation, such interactions are clearly observed. It appears that the ethylidene group, which is present at position C-10 in **11a**, is not bulky enough to provide sufficient steric hindrance for such a dramatic conformational change. However, the acyl intermediate of **11a** is stabilized against hydrolysis through favorable conjugation of the acyl carbonyl with the ethylidene group, which is pointed toward residues Leu 119

and Gln 120.¹⁵ Similar resonance stabilization effects have also been described for cephem sulfone⁴³ and penem inhibitors⁴⁴ of β -lactamases.

Proposed Inhibition Mechanism in Class C β -Lactamases.

The catalytic water molecule, which is responsible for deacylation of enzyme–substrate covalent intermediates and is observed in several class C β -lactamase complexes,^{39–41} is not present in the AmpC/**11a** complex structure. Since the bicyclic ring of the intermediate **11a** itself is not able to completely block the approach of a water molecule to the acyl ester bond, rotation of the opened β -lactam ring of **11a** about the C9–C10 and/or C10–C11 bonds (Figure 1) upon acylation appears to be responsible for displacement of the putative deacylating water molecule. The crystal structure of acyl-enzyme intermediate for imipenem bound to TEM-1 β -lactamase from *E. coli* indicates a conformational change for the complex which supposedly

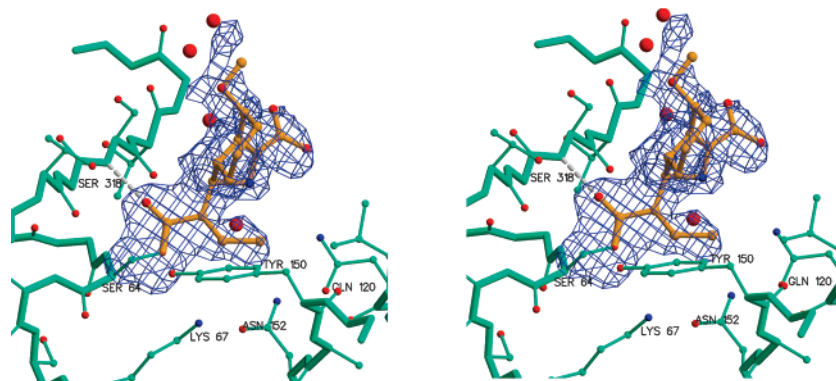


Figure 3. P99 β -lactamase from the *E. cloacae* active-site with bound inhibitor **11a** in stereoview (a, left; b, right). The β -lactamase is presented in cyan, and main chain bonds are thicker. The inhibitor is drawn in orange. The nitrogen atoms are colored blue, and oxygen atoms red. The hydrogen bond between the inhibitor and the enzyme is shown in gray. $2F_o - F_c$ electron density map (inhibitor atoms only) at 2.05 Å resolution is contoured at 0.8 σ . The image was generated by programs Raster3d⁵² and MAIN.⁵⁴ PDB ID entry code of the structure is 2Q9M.

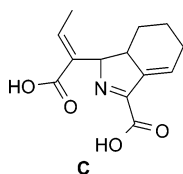


Figure 4. The structure of the intermediate C after deacylation by Ser 64 of β -lactamase.¹⁷

accounts for the ability of the antibiotic to resist hydrolytic deactivation by β -lactamase.⁴⁵

In our previous study,¹⁷ we showed that the product from the β -lactamase-catalyzed and basic hydrolysis of compound **11a** is intermediate C (Figure 4), where tautomerization of the cleaved β -lactam ring and elimination of the 4-methoxy group has occurred. This behavior was previously documented for other β -lactams, such as cephalosporins⁴³ and oxacephem,⁴⁴ with the leaving group at position C3.

In the case of our covalently bound trinem complex the electron density of the 4-methoxy group, which is clearly observed in the acylated complex, indicates that the acylation process cannot be accompanied by the simultaneous elimination of the 4-methoxy group, at least for **11a** under these particular crystallization conditions. Our crystallographic data corroborates, that in the case of **11a**, elimination of the leaving methoxy group proceeds only after the deacylation step and release of the product from the enzyme is completed.

Structure–Activity Relationship of Novel Trinem Inhibitors. Recently, the paradigm of rational drug design has shifted its focus from optimization of *in vitro* enzymatic inhibitory activity toward accounting for ADME properties of the inhibitors.⁴⁶ Thus, in order to vary the lipophilic character of the lead compound **11a** we exploited the details of its crystal structure in the complex with the enzyme. Since the oxygen atom of the 4-methoxy group of compound **11a** forms no interactions with the active site and at the same time the methyl moiety is exposed to the solvent, we hypothesized that position 4 would be suitable for balancing the lipophilicity while maintaining inhibitory activity (Table 1). Compounds **11b–h** were designed to test this hypothesis, and their lipophilic character was predicted by calculating the octanol/water partition coefficient.⁴⁷ Rather conservative substitutions at position 4 offered a spread of 2 log units in log P values. With the exception of the fluoroethoxy derivative **11g** (log $P_{\text{calc}} = 0.97$; log $D_{\text{calc}} = -1.82$) all the compounds possess higher calculated log P and log D (pH = 7.4) values compared to the parent compound **11a** (log $P_{\text{calc}} = 1.28$; log $D_{\text{calc}} = -1.48$), whereas compounds **11e** and **11f** are the most lipophilic in the series.

The results of the inhibitory activities evaluations against class A (TEM-1 and SHV-1 from *Escherichia coli*) and class C (AmpC from *E. cloacae*) β -lactamases for compounds **11a–h** are presented in Table 2 and are compared to clavulanate⁴⁸ and tazobactam.⁴⁹ The *in vitro* activities of these compounds against class A enzymes are comparable to clavulanate and tazobactam. In contrast, significant improvement of potency by 2–30-fold compared to tazobactam and 100–2000-fold compared to clavulanate was achieved against the representative class C enzyme AmpC with **11a** being the most potent inhibitor.

Surprisingly, and contrary to our hypothesis, the IC₅₀ values of compounds **11b–h** against class C β -lactamase AmpC were 3–16-fold higher compared to the lead compound **11a**. On the other hand, introduction of bulkier substituents at position 4 roughly preserved the *in vitro* activity of compounds **11b–h** against class A β -lactamases. Similarly, our initial hypothesis based on the structure of the complex AmpC/**11a** that a structural change at position 4 such as introduction of fluorine (**11g**) or cyano group (**11h**) on an ethoxy spacer would enable additional favorable electrostatic contacts with the enzyme surface did not yield any beneficial effect to binding of these derivatives.

Furthermore, four compounds, **11b**, **11e**, **11g**, and **11h**, exhibit a 3-fold increase in potency against TEM-1 enzyme compared to **11a**. In the case of TEM-1 enzyme the (4*R*,8*R*)-stereoisomer of the ethoxy and butoxy derivatives is twice as potent as the (4*S*,8*S*)-stereoisomer. This pattern of stereoselectivity, which is not completely preserved for SHV-1 and AmpC enzymes, might be useful for further improvement of trinem inhibitory activity.

Two possibilities to explain the somewhat unexpected diminished AmpC inhibitory activities in this series could be suggested: (i) the preferred conformation in compounds **11b–h** in the acyl-AmpC complex is different from the observed conformation of **11a**. Alternatively, (ii) the acyl intermediate conformations are similar to the determined crystal structure of the complex, but the bulkier substituents at position C-4 might not be favorably positioned in the previous step of the catalytic process, i.e., when the noncovalent Michaelis complex is formed and after subsequent reorganization in the active site upon acylation. Preliminary docking studies (unpublished results from this laboratory)⁵⁰ of the noncovalently bound compounds from this series in the AmpC active site indicate that the lipophilic substituents at position C-4 of the trinem structure are directed toward the segment of residues 280–295. This part of the binding site has previously been observed to be conformationally disordered in some crystal structures of AmpC β -lactamases.^{43,44}

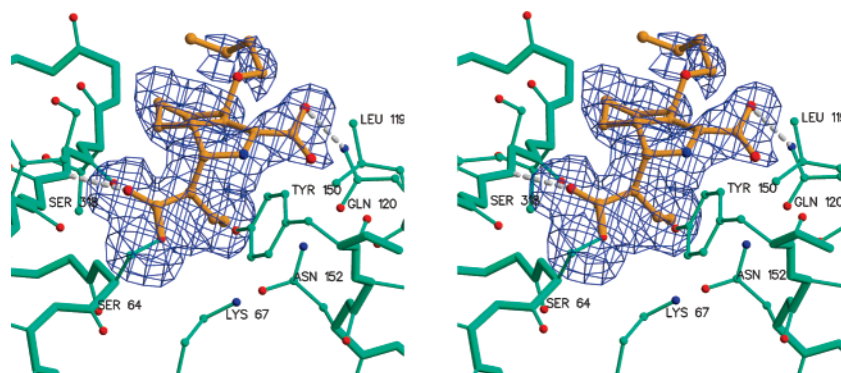


Figure 5. P99 β -lactamase from *E. cloacae* active site with bound inhibitor **11e** in stereoview (a, left; b, right). $2F_o - F_c$ electron density map (inhibitor atoms only) at 2.20 Å resolution is contoured at 0.8σ . Details same as in Figure 3. PDB ID entry code of the structure is 2Q9N.

Table 1. Stereoisomerism of the Intermediates **2a–9h** and Final Compounds **11a–h**^a

compound	R	compound	R	compound	R
2a	R = Me	4a, 7a	(1 <i>R</i> ,3 <i>S</i>)	8a, 9a, 10a, 11a	(4 <i>S</i> ,8 <i>S</i>)
2b	R = Et	4b, 7b	(1 <i>S</i> ,3 <i>R</i>)	8b, 9b, 10b, 11b	(4 <i>R</i> ,8 <i>R</i>)
		4c, 7c	(1 <i>R</i> ,3 <i>S</i>)	8c, 9c, 10c, 11c	(4 <i>S</i> ,8 <i>S</i>)
2c	R = iPr	4d, 7d	(1 <i>R</i> ,3 <i>S</i>)	8d, 9d, 10d, 11d	(4 <i>S</i> ,8 <i>S</i>)
2d	R = Bu	4e, 7e	(1 <i>S</i> ,3 <i>R</i>)	8e, 9e, 10e, 11e	(4 <i>R</i> ,8 <i>R</i>)
		4f, 7f	(1 <i>R</i> ,3 <i>S</i>)	8f, 9f, 10f, 11f	(4 <i>S</i> ,8 <i>S</i>)
		6g, 4g, 7g	(1 <i>R</i> ,3 <i>S</i>)	8g, 9g, 10g, 11g	(4 <i>S</i> ,8 <i>S</i>)
		6h, 4h, 7h	(1 <i>R</i> ,3 <i>S</i>)	8h, 9h, 10h, 11h	(4 <i>S</i> ,8 <i>S</i>)
			R = Me		R = Me
			R = Et		R = Et
			R = Et		R = Et
			R = iPr		R = iPr
			R = Bu		R = Bu
			R = Bu		R = Bu
			R = (CH ₂) ₂ F		R = (CH ₂) ₂ F
			R = (CH ₂) ₂ CN		R = (CH ₂) ₂ CN

^a (4*R*,8*R*) isomer of 4-OiPr analogue was not prepared with sufficient purity and is therefore not included.

Table 2. *In Vitro* Activity and Calculated Partition Coefficients of Compounds **11a** and **11b–h** against Class A (TEM-1 and SHV-1) and Class C (AmpC) β -Lactamases

compound	IC ₅₀ [μ M] ^a			calculated partition coefficient ^b	
	TEM-1	SHV-1	AmpC	log P_{calc}	log D_{calc} (pH 7.4)
clavulanate	0.030	0.028	136.2	-1.98	-5.68
tazobactam	0.017	0.222	1.808	-1.70	-5.43
11a ^c	0.055	0.151	0.062	1.28	-1.48
11b	0.022	0.284	0.295	1.81	-0.94
11c	0.057	0.385	0.229	1.81	-0.94
11d	0.039	0.340	0.341	2.16	-0.58
11e	0.012	0.219	0.430	2.88	0.12
11f	0.032	0.206	0.720	2.88	0.12
11g	0.021	0.148	1.020	0.97	-1.82
11h	0.018	0.152	0.209	1.42	-1.36

^a IC₅₀ values are presented as an average of at least two measurements with variability of 0.1 units. ^b log P and log D (at pH 7.4) were calculated using ACD/Labs7.0 software. ^c Lead compound **11a**.

Under our conditions for crystallization of AmpC from *E. cloacae* with **11a** only one monomer is located in an asymmetric unit. However, in other crystal structures of AmpC from *E. coli* in complex with various ligands two monomers were observed in each asymmetric unit.⁵¹ While monomer 2 always adopts a similar conformation to that observed in our complex (rmsd for all backbone atom pairs is ~ 0.5 Å) the main difference is located in monomer 1 in which residues 280–295 are disordered and its structure could not be determined. Similarly, Lobkovsky et al.⁵¹ have observed positional disorder of the tetrahedral phosphonate derivative intermediate in the complex with *E. cloacae* P99 cephalosporinase. Their seminal observation in this respect was that the difference in active site volume available for specific ligand binding between class A and class C β -lactamase enzymes might be accounted for by the unexpected position of the β -lactam carbonyl in the observed acyl tetrahedral intermediate in class C β -lactamase enzyme.

To resolve these issues we have determined the crystal structure of the 4-OBu derivative (compound **11e**) which has

increased lipophilicity compared to parent compound **11a** (as estimated by log P value of 2.88) with AmpC β -lactamase. It was found that the 4-butyloxy substituent is exposed toward solvent in a similar way to 4-OMe substituent (Figure 5). Thus, on one hand, the notion of the unfavorable energetic influence of a more lipophilic substituent exposed to solvent for an inhibitory constant of compound **11e** which is weakened by a factor of 7 (0.430 nmol) compared to 62 nmol for compound **11a** appears to be correct. On the other hand, this crystal structure enables answer to the question: is the effect of lipophilic functionality at position 4 of the trinem negligible? By comparing both solved crystal structures, we are in position to describe the variation in the interaction pattern in compounds **11e** and **11a**. The interactions of the covalently bound β -lactam fragment of the trinem scaffold with residues Ser 64, Lys 67, and Ser 318 of the active site are very similar. The carboxylate substituents are oriented toward lipophilic environment of Leu 119 and Gln 120 in both compounds, and the bulky trinem rings B and C are positioned in the enzymatic cleft. Most interestingly, both C4 substituents are exposed to solvent. This similarity leads us to the conclusion that the introduction of a bulkier C4 substituent in compound **11e** probably interacts unfavorably with the loop 280–295 in the noncovalent Michaelis complex formed before reorganization in the active site upon acylation step. This appears to be responsible for the unfavorable change in the binding and weakening the effect of an additional hydrogen bond between carboxylate group of compound **11e** with backbone amide of Gln 120 as well.

Conclusions

The compound **11a** was previously identified as a promising candidate for a β -lactamase inhibitor in bacterial infections which show resistance to currently available antibiotics. A series of analogues of our lead compound **11a** with a variety of substituents at position C4 was synthesized and evaluated.

Potency of the derivatives compared to **11a** decreased, however, some of the compounds still maintain interesting inhibitory activity to both class A and class C β -lactamase

enzymes. The variations in lipophilicity of the derivatives in the series offers possibilities for optimization of pharmacokinetic properties. Although we cannot confirm this hypothesis as yet, it is reasonable to expect that changing $\log P$ and $\log D$ in the series would enable optimization of properties such as clearance.

The solved crystal structures of the inhibitors **11a** and **11e** in complexes with enzyme AmpC from *E. cloacae* P99 provide a viable rationale for further cycles of rational structure-based design of the first tricyclic carbapenem inhibitor of β -lactamases.

Experimental Section

Enzymatic Assays. Assays were performed with β -lactamases expressed in the pET system (Novagen, San Diego, CA) without signal peptides. They contained an N-terminal hexahistidine tag that was used for purification on Ni-NTA resin (Qiagen, Hilden, Germany). Compounds were prepared as 50 mM stocks in DMSO and diluted with buffer P1 (50 mM phosphate, pH 7) to a final concentration of 10% DMSO. All further dilutions were done using P2 (P1 with 10% DMSO). Enzyme and compound dilutions were preincubated for 10 min at 37 °C, and the reaction started with the addition of prewarmed (37 °C) nitrocefin at a final concentration of 50 mM. The change in absorption at 490 nm was followed at 37 °C for 10 min at 30 s intervals in a Spectramax 384 Plus microplate reader (Molecular Devices, Sunnyvale, CA) using 96-well plates. The initial rate was determined, and IC_{50} values were calculated using nonlinear regression and sigmoidal dose–response analysis with the PRISM 4.0 software (Graphpad Software Inc., San Diego, CA). IC_{50} data is expressed as μ M within the 95% confidence interval (95% CI) and was calculated from at least two independent experiments.

Crystal Growth and Structure Determination. (a) β -Lactamase–11a Complex. The crystals of AmpC β -lactamase were grown by vapor diffusion method by hanging 2 μ L drops of precipitant and protein solution over a solution of 22% PEG 4000, 0.1 M Na acetate at pH 4.8, and 0.2 M ammonium acetate. Crystals of the size 0.1 \times 0.1 \times 0.5 mm grew in 3–4 weeks at 19 °C and were suitable for cryodata collection. A solution of 50 mM inhibitor was prepared using INH buffer (22% Peg4000, 10% glycerol, 0.1 M Na acetate pH 7.0, 0.2 M ammonium acetate). Soaking was performed just before the measurement in 1 μ L drops on glass. Crystals were soaked at 21 \times bcC for 2.5 h. Subsequently, the solution containing inhibitor was replaced and soaking continued for another 2.5 h. Crystals prepared as described were frozen in liquid nitrogen.

(b) Diffraction Data Collection. The crystal diffracted to 2.0 Å resolution in the space group $P2_12_12$ with unit cell parameters $a = 76.65$ Å, $b = 69.77$ Å, and $c = 62.82$ Å, $\alpha = \beta = \gamma = 90$. The AmpC structure of the apoenzyme was used as a starting structure,⁵³ and the inhibitor was modeled in the active site. The data set of 20733 reflections (96.8% complete) were collected at XRD-1 beam line at Elettra Synchrotron Facility in Trieste at 100 K using 162 mm MAR CCD detector. Frames were counted over 0.75 \times bc oscillation images for 40 s. There were total of 112 images over 84 \times bc range. The reflections were indexed, integrated, and scaled using the HKL2000 software suite.⁵³

(c) Structure Determination of the Enzyme–11a Complex. Molecular replacement was solved using the AMoRe program with one molecule in units and an R factor of 25.4 and correlation coefficient of 60.0. The model of P99 β -lactamase with PDB ID 1XX2 was loaded into program suite MAIN.⁵⁴ Several cycles of model fitting and refinement were carried out using the Engh and Huber parameter set.⁵⁵ The resulting electron density difference maps clearly revealed the presence of inhibitor covalently bound to the reactive site Ser 64. Water molecules were added, and resolution of the data was gradually extended to maximum 2.05 Å. The final crystallographic R factor is 0.209 and R_{symm} is 0.121. The final model of the enzyme–inhibitor complex was composed of 3282 proteins, 19 atoms of inhibitor **11a**, and 367 crystal water molecules.

Interestingly, the space group and unit cell dimensions are not similar to P99 β -lactamase's crystals determined previously (PDB code 1XX2⁵⁶) but are closer to the values of *E. cloacae* GC1 β -lactamase crystals (PDB ID code 1GCE,⁵⁷ Although the crystal dimensions are similar, there is no density space between Asp 205 and Lys 207 for insertion of three additional amino acids present in the GC1 β -lactamase sequence. Results are presented in Table S2 of the Supporting Information.

(d) β -Lactamase–11e Complex. The protein (AmpC β -lactamase) was cloned with the purification His-tag attached. It was linked via a thrombin cleavage site linker consisting of six residues (LVPR†GS) which was removed prior to crystallization. PBS was used as the cleavage buffer (140 mM NaCl, 2.7 mM KCl, 10 mM Na_2HPO_4 , 1.8 mM KH_2PO_4 , pH = 7.3). Thrombin was prepared as a stock solution by dissolving 250 U of thrombin into 250 μ L of PBS buffer. Cleavage was performed at 19 \times bcC for 24 h. Further cleavages were blocked with addition of 0.5 μ L of PMSF, a thrombin irreversible inhibitor. After 30 min, the excess PMSF and cleaved His-Tag were removed by dialysis on MICROCON using a 3000 Da membrane.

The crystals were grown by the hanging drop vapor diffusion method with a solution of 22% PEG4000, 0.1 M Na acetate at pH 4.8, 0.2 M ammonium acetate. Crystals of the size 0.1 \times 0.2 \times 0.5 mm appeared within 14 to 21 days and were suitable for cryodata collection. They belonged to $P2_12_12$ space group with unit cell dimensions $a = 77.33$ Å, $b = 68.98$ Å, $c = 62.02$ Å, $\alpha = \beta = \gamma = 90$ and contained a single molecule per asymmetric unit.

Solution of (~50 mM) inhibitor was prepared in INH buffer (22% PEG4000, 10% glycerol, 0.1 M Na acetate pH = 7.0, 0.2 M ammonium acetate). Soaking was performed just before the measurement in 1 μ L drops on glass. During a 4 h soak, the solution was exchanged three times. The crystals were transferred into a liquid nitrogen stream and exposed to X-rays immediately after the soaking.

X-ray diffraction data were collected in-house at a RIGAKU RU-200 rotating anode (Cu, $\lambda = 1.5418$ Å) at 100 K using a MAR345 IP detector. Frames were counted over 1 \times bc oscillation images for 600 s. There were a total of 100 images over a 100 \times bc range. The reflections were indexed, integrated, and scaled using the HKL2000 software suite.⁵³ Results are presented in Table S2 of the Supporting Information.

(e) Structure Determination of the Enzyme–11e Complex. The previously determined structure of the AmpC β -lactamase molecule was used for the starting model. The final R factor was 0.252 using diffraction data in the resolution range 10–2.2 Å. The structure of inhibitor **11e** was clearly visible in the final electron density map. The orientation of the **11e** is different from the **11a** structure. The difference in orientation is presumably a consequence of the larger nonpolar side chain present in **11e**.

General Chemical Methods. Analytical TLC was performed on Merck silica gel 60 F₂₅₄ plates (0.25 mm), and the components detected using specific spray reagents. Column chromatography was carried out on silica gel 60 (particle size 240–400 mesh). Melting points were determined on a Reichert hot stage microscope and are uncorrected or obtained from DSC spectra, which were recorded on a Mettler Toledo DSC822e. IR spectra were obtained with a Nicolet FT-IR Nexus spectrometer and optical rotation was measured on a Perkin-Elmer 1241 MC polarimeter. ¹H NMR spectra were recorded on a Varian Inova300 spectrometer in CDCl₃ or DMSO-*d*₆ solution, with TMS as the internal standard. Mass spectra were obtained using a VG-Analytical Autospec Q mass spectrometer. HPLC analyses were performed using a Waters 2695 Separation Module with a Waters 2996 PDA detector and an XTerra RP C18 (150 \times 4.6 mm I.D., 3.5 μ m particle size) analytical column and a gradient elution method combining mobile phase A with 25 mM ammonium acetate (pH = 6)/acetonitrile (95/5 v/v) and mobile phase B with 25 mM ammonium acetate (pH = 6)/acetonitrile (10/90 v/v). LC-MS analyses were performed on an Alliance HT Waters 2795 separations module with a Waters 2996 (photodiode array) UV-detector and a Micromass Quatro Micro mass spectrometer. HRMS analyses were performed on Micromass QTOF Ultima

Global using ESI (negative and positive mode). All reported yields are yields of purified products. Alternative additional HPLC analyses were performed (denoted as method 1 below) using Agilent 1100 Separation Module and Luna C18 (250 \times 4.6 mm I.D., 5 mm particle size) analytical column by an isocratic elution method combining 25 mM ammonium phosphate buffer (pH = 7.57)/acetonitrile (60/40 v/v).

General Procedure F. Synthesis of Sodium (8S/ 8R,9R)-10-(E)-Ethylidene-4(S/ R)-alkoxy-11-oxo-1-azatricyclo[7.2.0.0^{3,8}]-undec-2-encarboxylate (11a–h). Compounds **10a–h** were prepared according to general procedures A–E described in the Supporting Information. PPh₃ (42.6 mg, 1.63 mmol, 0.1 equiv), Pd(PPh₃)₄ (43.1 mg, 0.041 mmol, 0.025 equiv), and 0.21 M sodium 6-ethylhexanoate solution in THF (NaEH) (7.8 mL, 1.63 mmol, 1 equiv) were added during stirring into a solution of **10a–h** (1.63 mmol, 1 equiv) in THF (10 mL). The mixture was left stirring at room temperature until complete conversion was detected. If the product precipitated from the reaction mixture spontaneously or after the addition of diethyl ether or petroleum ether, it was filtered off and dried. Otherwise, water (30 mL) was added, washed (3 \times 10 mL) with ethyl acetate, and lyophilized.

Sodium (8S,9R)-10(E)-Ethylidene-4(S)-methoxy-11-oxo-1-azatricyclo[7.2.0.0^{3,8}]-undec-2-encarboxylate (11a). Compound **11a** was prepared from **10a** according to General Procedure F. The obtained product was precipitated from the reaction mixture; yield 90.0%, white amorphous powder; mp 151–152 °C; [α]_D²⁰ (H₂O, 10.0 mg/mL) = +100.0. IR (KBr) ν [cm⁻¹] 2934, 1763, 1609, 1397, 1189, 1088, 959, 779. ¹H NMR (DMSO-*d*₆) δ [ppm] 1.00–1.64 (m, 6H), 1.80 (d, 3H, *J* = 7.2 Hz, CH₃CH=), 3.00–3.09 (m, 1H), 3.11 (s, 3H, OCH₃), 4.60 (d, 1H, *J* = 10.4 Hz, H-9), 5.12 (t, 1H, *J* = 2.7 Hz, H-4), 6.29 (dq, 1H, *J*₁ = 7.0 Hz, *J*₂ = 1.5 Hz, CH₃CH=). ¹³C NMR (DMSO-*d*₆) δ [ppm] 14.7, 20.1, 30.1, 31.8, 43.4, 54.8, 59.8, 72.0, 126.7, 134.0, 136.0, 140.2, 164.4, 170.9. HRMS ([M – Na]⁻): Anal. calcd for C₁₄H₁₆NO₄: 262.1079; found: 262.1086. HPLC purity: 99.55 area%. HPLC purity (method 1): 100%.

Sodium (8R,9R)-10(E)-Ethylidene-4(R)-ethoxy-11-oxo-1-azatricyclo[7.2.0.0^{3,8}]-undec-2-encarboxylate (11b). Compound **11b** was prepared from **10b** according to General Procedure F. The obtained product was precipitated from the reaction mixture to give **11b**; yield: 63.4%, yellow amorphous solid; mp decomp above 160 °C; [α]_D²⁰ (H₂O, 1.065 mg/mL) = +10.2. IR (KBr) ν [cm⁻¹] 3439, 2971, 2932, 2863, 1754, 1594, 1391, 1228, 1194, 1070. ¹H NMR (DMSO-*d*₆) δ [ppm] 1.02 (t, 3H, *J* = 7.0 Hz, CH₃CH₂O), 1.74 (d, 3H, *J* = 7.0 Hz, CH₃CH=), 1.22–1.33 (m, 2H), 1.42–1.46 (m, 1H), 1.56–1.65 (m, 1H), 1.78–1.83 (m, 1H), 2.05–2.11 (m, 1H), 2.83–2.92 (m, 1H, H-8), 3.27–3.45 (m, 2H, CH₃CH₂O), 4.01 (d, 1H, *J* = 7.2 Hz, H-9), 5.15 (brs, 1H, H-4), 6.18 (dq, 1H, *J* = 7.1 Hz, 1.5 Hz, CH₃CH=). ¹³C NMR (DMSO-*d*₆) δ [ppm] 14.7 (CH₃CH=), 15.6 (CH₃CH₂O), 19.4 (C-6), 31.8 (C-5), 34.2 (C-7), 43.9 (C-8), 61.9 (CH₃CH₂O), 63.4 (C-9), 68.7 (C-4), 125.6 (CH₃CH=), 133.1 (C-3), 137.0 (C-2), 142.9 (C-10), 164.3 (COOK), 170.8 (C=O). HRMS ([M – Na]⁻): Anal. calcd for C₁₅H₁₈NO₄: 276.1236; found: 276.1227. HPLC purity: 98.02 area%. HPLC purity (method 1): 99.9%.

Sodium (8S,9R)-10(E)-Ethylidene-4(S)-ethoxy-11-oxo-1-azatricyclo[7.2.0.0^{3,8}]-undec-2-encarboxylate (11c). Compound **11c** was prepared from **10c** according to General Procedure F. The obtained product was precipitated from the reaction mixture after the addition of diethyl ether and petroleum ether to give **11c**; yield: 19.2%, yellow amorphous powder; mp decomp above 180 °C, [α]_D²⁰ (H₂O, 1.04 mg/mL) = +75.5. IR (KBr) ν [cm⁻¹] 3456, 2931, 1753, 1606, 1396, 1236, 1090, 1071. ¹H NMR (DMSO-*d*₆) δ [ppm] 1.07 (t, 3H, *J* = 7.0 Hz, CH₃CH₂O), 0.99–1.13 (m, 1H), 1.22–1.32 (m, 1H), 1.41–1.45 (m, 1H), 1.58–1.81 (m, 3H), 1.76 (dd, 3H, *J*₁ = 7.0 Hz, *J*₂ = 0.6 Hz, CH₃CH=), 2.96–3.06 (m, 1H, H-8), 3.24–3.37 (m, 2H, CH₃CH₂O), 4.58 (d, 1H, *J* = 10.1 Hz, H-9), 5.22 (t, 1H, *J* = 2.7 Hz, H-4), 6.28 (dq, 1H, *J*₁ = 7.1 Hz, *J*₂ = 1.6 Hz, CH₃CH=). ¹³C NMR (DMSO-*d*₆) δ [ppm] 14.7 (CH₃CH=), 15.5 (CH₃CH₂O), 20.2 (C-6), 30.2 (C-5), 32.1 (C-4), 43.5 (C-8), 59.7 (CH₃CH₂O), 62.1 (C-9), 70.0 (C-4), 126.6 (CH₃CH=), 134.7 (C-3), 135.6 (C-2), 140.2 (C-10), 164.4 (COONa),

170.9 (C=O). HRMS ([M – Na]⁻): Anal. calcd for C₁₅H₁₈NO₄: 276.1236; found: 276.1246. HPLC purity: 98.00 area%. HPLC purity (method 1): 99.9%.

Sodium (8S,9R)-10(E)-Ethylidene-4(S)-isopropoxy-11-oxo-1-azatricyclo[7.2.0.0^{3,8}]-undec-2-encarboxylate (11d). Compound **11d** was prepared from **10d** according to General Procedure F. The obtained product was precipitated from the reaction mixture after the addition of diethyl ether to give **11d**; yield: 21.7%, yellow amorphous powder; mp decomp above 160 °C; [α]_D²⁰ (H₂O, 1.055 mg/mL) = +40.5. IR (KBr) ν [cm⁻¹] 3439, 2931, 1752, 1634, 1395, 1018. ¹H NMR (DMSO-*d*₆) δ [ppm] 1.04 (t, 3H, *J* = 5.3 Hz, CH₃-CH₂O), 1.05 (t, 3H, *J* = 5.3 Hz, CH₃CH₂O), 1.75 (d, 3H, *J* = 7.2 Hz, CH₃CH=), 1.22–1.32 (m, 1H), 1.39–1.44 (m, 1H), 1.60–1.74 (m, 4H), 2.96–3.06 (m, 1H, H-8), 3.46–3.55 (m, 2H, CH₃CH₂O), 4.55 (d, 1H, *J* = 10.1 Hz, H-9), 5.32 (t, 1H, *J* = 2.9 Hz, H-4), 6.24 (dq, 1H, *J*₁ = 7.1 Hz, *J*₂ = 1.6 Hz, CH₃CH=). ¹³C NMR (DMSO-*d*₆) δ [ppm] 14.7 (CH₃CH=), 20.1 (CH₃CH₂O), 23.6 (C-6), 30.3 (C-5), 32.6 (C-7), 43.5 (C-8), 59.7 (CH₃CH₂O), 66.9 (C-9), 76.5 (C-4), 126.5 (CH₃CH=), 135.2 (C-3), 135.6 (C-2), 140.2 (C-10), 164.4 (COONa), 170.8 (C=O). HRMS ([M – Na]⁻): Anal. calcd for C₁₆H₂₀NO₄: 290.1392; found: 290.1384. HPLC purity: 98.86 area%. HPLC purity (method 1): 98.45%.

Sodium (8R,9R)-10(S)-[1(R)-Hydroxyethyl]-4(R)-butoxy-11-oxo-1-azatricyclo[7.2.0.0^{3,8}]-undec-2-encarboxylate (11e). Compound **11e** was prepared from **10e** according to General Procedure F. The obtained product was precipitated from the reaction mixture; yield: 66.0%, white crystals; mp 181 °C, [α]_D²⁰ (H₂O, 1.045 mg/mL) = +59.1. IR (KBr) ν [cm⁻¹] 1102, 1219, 1390, 1595, 1757, 2861, 2939, 3439. ¹H NMR (DMSO-*d*₆): δ 0.80 (t, 3H, *J* = 7.3, CH₃-(CH₂)₃O), 1.18–1.83 (m, 10H), 1.73 (dd, 3H, *J* = 7.1, 0.8, CH₃CH=), 2.01–2.12 (m, 1H), 2.80–2.92 (m, 1H, H-9), 3.24–3.41 (m, 2H, OCH₂(CH₂)₂CH₃), 4.07 (d, 1H, *J* = 7.0 Hz, H-9), 5.10 (deg. dd, 1H, *J* = 2.6 Hz, H-4), 6.16 (dq, 1H, *J* = 7.0, 1.5 Hz, CH₃CH=). ¹³C NMR (75 MHz, DMSO-*d*₆): δ 14.5, 14.6, 18.9, 19.4, 31.6, 31.8, 34.2, 43.9, 63.3, 66.0, 67.0, 68.8, 125.4, 133.3, 136.8, 142.9, 164.35, 170.90. MS (M + H)⁺ = 328 m/z. HRMS ([M – Na]⁻): Anal. calcd for C₁₇H₂₂NO₄: 304.1549; found: 304.1563. HPLC purity: 98.69 area%. HPLC purity (method 1): 98.76%.

Sodium (8S,9R)-10(S)-[1(R)-Hydroxyethyl]-4(S)-butoxy-11-oxo-1-azatricyclo[7.2.0.0^{3,8}]-undec-2-encarboxylate (11f). Compound **11f** was prepared from **10f** according to General Procedure F. The reaction mixture was dissolved in 50 mL of H₂O and washed with 2 \times 25 mL CH₂Cl₂. The product was obtained after lyophilization; yield 36.9%, white-yellow crystals; mp 195 °C, [α]_D²⁰ (H₂O, 1.045 mg/mL) = +47.7. IR (KBr) ν [cm⁻¹] 1092, 1396, 1599, 1751, 2863, 2932, 3439. ¹H NMR (DMSO-*d*₆): δ 0.86 (t, 3H, *J* = 7.3 Hz, CH₃-(CH₂)₃O), 0.98–1.85 (m, 10H), 1.76 (d, 3H, *J* = 7.1 Hz, CH₃-CH=), 2.95–3.08 (m, 1H, H-9), 3.20–3.40 (m, 2H, OCH₂(CH₂)₂-CH₃), 4.59 (d, 1H, *J* = 10.1 Hz, H-9), 5.20 (t, 1H, *J* = 2.8 Hz), 6.28 (dq, 1H, *J*₁ = 7.1, *J*₂ = 1.6 Hz, CH₃CH=). ¹³C NMR (75 MHz, DMSO-*d*₆): δ 13.8, 14.7, 19.0, 20.1, 30.2, 31.8, 32.1, 43.5, 59.7, 66.4, 70.2, 126.6, 134.9, 135.4, 140.1, 164.4, 170.9. HRMS ([M – Na]⁻): Anal. calcd for C₁₇H₂₂NO₄: 304.1549; found: 304.1558. HPLC purity: 97.03 area%. HPLC purity (method 1): 96.81%.

Sodium (8S,9R)-10(E)-Ethylidene-4(S)-(2'-fluoroethoxy)-11-oxo-1-azatricyclo[7.2.0.0^{3,8}]-undec-2-encarboxylate (11g). Compound **11g** was prepared from **10g** according to General Procedure F. The product was precipitated from the reaction mixture; 37% yield; white amorphous powder; mp decomp above 194 °C; [α]_D²⁰ (H₂O, 1.055 mg/mL) = +89.0. ¹H NMR (DMSO-*d*₆) δ [ppm] 1.08 (m, 1H), 1.30 (m, 1H), 1.47 (m, 1H), 1.60–1.86 (m, 3H), 1.77 (d, *J* = 7.2 Hz, 3H, CH₃CH=), 3.03 (m, 1H), 3.47 (m, 1H), 3.57 (m, 1H), 4.41 (m, 1H), 4.58 (m, 1H), 4.60 (d, *J* = 10.5 Hz, 1H, H-9), 5.30 (t, *J* = 2.60 Hz, 1H, H-4), 6.31 (dd, *J*₁ = 7.2, *J*₂ = 1.7 Hz, 1H, CH₃CH=). ¹³C NMR (DMSO-*d*₆) δ [ppm] 14.7, 20.0, 30.0, 31.9, 43.3, 59.8, 66.3 (*J* = 19 Hz), 70.5, 82.8 (*J* = 165 Hz), 127.0, 134.1, 135.6, 140.1, 164.4, 171.0. HRMS ([M – Na]⁻): Anal. calcd

for C₁₅H₁₇NO₄F: 294.1136; found: 294.1142. HPLC purity: 98.2 area%. HPLC purity (method 1): 99.9%.

Sodium (8S,9R)-10(E)-Ethylidene-4(S)-(2'-cyanoethoxy)-11-oxo-1-azatricyclo[7.2.0.0^{3,8}]undec-2-encarboxylate (11h). Compound **11h** was prepared from **10h** according to General Procedure F. The product was precipitated from the reaction mixture; 79% yield; white amorphous powder; mp decomp above 188 °C. [α]_D²⁰ (H₂O, 1.075 mg/mL) = +58.6. ¹H NMR (DMSO-*d*₆) δ [ppm] 1.04–1.85 (m, 6H), 1.78 (d, *J* = 7.0 Hz, 3H, CH₃CH=), 2.80 (m, 2H), 3.08 (m, 1H), 3.48 (m, 2H), 4.63 (d, *J* = 10.2 Hz, 1H, H-9), 5.34 (t, *J* = 2.6 Hz, 1H, H-4), 6.32 (qd, *J*₁ = 1.6, *J*₂ = 7.0 Hz, 1H, CH₃CH=). ¹³C NMR (DMSO-*d*₆) δ [ppm] 14.7, 17.9, 20.0, 29.9, 31.9, 43.3, 59.7, 61.9, 70.1, 119.4, 127.1, 133.7, 136.2, 140.0, 164.2, 171.0. HRMS ([M – Na]⁺): Anal. calcd for C₁₆H₁₇N₂O₄: 301.1188; found: 301.1181. HPLC purity: 97.0 area%. HPLC purity (method 1): 97.92%.

Acknowledgment. We gratefully acknowledge the technical expertise and contributions of Dr. Urška Bratušek-Zavadlal and Mr. B. Anžič. The authors thank the members of the Analytical group of Lek Pharmaceuticals d.d. for analytical and spectroscopic determinations. We are deeply indebted to Professor J. M. Frere and members of the Centre for Protein Engineering of the University Liege for their encouragement and continued help.

Supporting Information Available: Purity of compounds characterization data, details of data collection and structure refinement statistics, and general synthetic procedures A–E for preparation of intermediates **10a–h**. This material is available free of charge via the Internet at <http://pubs.acs.org>.

References

- Neu, H. C. The crisis in antibiotic resistance. *Science* **1992**, *257*, 1064–1073.
- Davies, J. Inactivation of antibiotics and dissemination of resistance genes. *Science* **1994**, *264*, 375–382.
- Frere, J. M. Beta-lactamases and bacterial resistance to antibiotics. *Mol. Microbiol.* **1995**, *16*, 385–395.
- Livermore, D. M. β -lactamase-mediated resistance and opportunities for its control. *J. Antimicrob. Chemother.* **1998**, *41*, 25–41.
- Jones, R. N.; Pfaller, M. A. Bacterial resistance: a worldwide problem. *Diagn. Microbiol. Infect. Dis.* **1998**, *31*, 379–388.
- Bush, K. Beta-lactamases of increasing clinical importance. *Curr. Pharm. Des.* **1999**, *5*, 839–845.
- Bush, K.; Jacoby, G. A.; Medeiros, A. A. A functional classification scheme for β -lactamases and its correlation with molecular structure. *Antimicrob. Agents Chemother.* **1995**, *39*, 1211–1233.
- Miller, L. A.; Ratnam, K.; Payne, D. J. β -lactamase-inhibitor combinations in the 21st century: current agents and new developments. *Curr. Opin. Pharmacol.* **2001**, *1*, 451–458.
- (a) Massova I.; Mobashery, S. Molecular bases for interactions between β -Lactam Antibiotics and β -Lactamases *Acc. Chem. Res.* **1997**, *30*, 162–168. (b) Massova, I.; Mobashery, S. Structural and Mechanistic Aspects of Evolution of β -Lactamases and Penicillin-Binding Proteins. *Curr. Pharm. Des.* **1999**, *5*, 929–937.
- Buynak, J. D. The discovery and development of modified penicillin and cephalosporin-derived β -lactamase inhibitors. *Curr. Med. Chem.* **2004**, *11*, 1951–1964.
- Bonnefoy, A.; Dupuis-Hamelin, C.; Steier, V.; Delamachume, C.; Seys, C.; Stachyra, T.; Fairly, M.; Guittion, M.; Lampilas, M. In vitro activity of AVE1330A, an innovative broad-spectrum non- β -lactam β -lactamase inhibitor. *J. Am. Chem. Soc.* **2004**, *54*, 410–417.
- Weiss, W. J.; Petersen, P. J.; Murphy, T. M.; Tardio, L. A.; Yang, Y.; Bradford, P. A.; Venkatesan, A. M.; Abe, T.; Isoda, T.; Mihira, A.; Ushigochi, H.; Takasake, T.; Projan, S.; O'Connell, J.; Mansour, T. S. In vitro and in vivo activities of novel 6-methylidene penems as β -lactamase inhibitors. *Antimicrob. Agents Chemother.* **2004**, *48*, 4589–4596.
- Phillips, O. A.; Czajkowski, D. P.; Spevak, P.; Singh, M. P.; Hanehara-Kunugita, C.; Hyodo, A.; Micetic, R. G.; Maiti, S. N. SYN-1012: A new β -lactamase inhibitor of penem skeleton. *J. Antibiot.* **1997**, *50*, 350–356.
- Jamieson, C. E.; Lambert, P. A.; Simpson, I. N. In vitro and in vivo activities of AM-112, a novel oxapenem. *Antimicrob. Agents Chemother.* **2003**, *47*, 1652–1657.
- Copar, A.; Prevec, T.; Anzic, B.; Mesar, T.; Selic, L.; Vilar, M.; Solmajer, T. Design, synthesis and bioactivity of tribactam β -lactamase inhibitors. *Bioorg. Med. Chem. Lett.* **2002**, *12*, 971–975.
- Copar, A.; Solmajer, T.; Anzic, B.; Kuzman, T.; Mesar, T.; Kocjan, D. Ethylidene Derivatives of Tricyclic Carbapenems. U.S. Patent 6,489,318, Dec 2002.
- Vilar, M.; Galleni, M.; Solmajer, T.; Turk, B.; Frere, J. M.; Matagne, A. Kinetic study of two novel enantiomeric tricyclic β -lactams which efficiently inactivate class C β -lactamases. *Antimicrob. Agents Chemother.* **2001**, *45*, 2215–2223.
- (a) Tamburini, B.; Perboni, A.; Rossi, T.; Donati, D.; Andreotti, D.; Gaviraghi, G.; Carlesso, R.; Bismara, C. EP 0416953B1; *Chem. Abstr.* **1991**, 116:235337. (b) Andreotti, D.; Rossi, T.; Gaviraghi, G.; Donati, D.; Marchioro, C.; Di Modugno, E.; Perboni, A. Synthesis and antibacterial activity of 4- and 8- methoxy trinems. *Bioorg. Med. Chem. Lett.* **1996**, *6*, 491–496. (c) Tranquillini, M. E.; Araldi, G. L.; Donati, D.; Pentassuglia, G.; Pezzoli, A.; Ursini, A. Synthesis and antimicrobial activity of 4-amino trinems. *Bioorg. Med. Chem. Lett.* **1996**, *6*, 1683–1688.
- (a) Iranpoor, N.; Salehi, P. Highly efficient, regio- und stereoselective alcoholysis of epoxides catalysed with iron (III) chloride. *Synthesis* **1994**, 1152–1154. (b) Piancatelli, G.; Scettri, A.; D'Auria, M. Pyridinium Chlorochromate: A Versatile Oxidant in Organic. *Synthesis* **1982**, 245–258.
- Rossi, T.; Marchioro, C.; Paio, A.; Thomas, R. J.; Zarantonello, P. Stereoselective synthesis of a key intermediate of Sanfetrinem by means of a chelated tin(IV) Enolate. *J. Org. Chem.* **1997**, *62*, 1653–1661.
- Marchioro, C.; Pentassuglia, G.; Perboni, A.; Donati, D. Synthesis and NMR studies of key intermediates to a new class of β -lactam: the trinems. *J. Chem. Soc., Perkin Trans. 1* **1997**, 463–468.
- (a) Andreotti, D.; Biondi, S.; Di, Fabio, R.; Donati, D.; Piga, E.; Rossi, T. Synthesis and biological evaluation of 4-alkoxy substituted trinems. Part I. *Bioorg. Med. Chem. Lett.* **1996**, *6*, 2019–2024. (b) Biondi, S.; Andreotti, D.; Rossi, T.; Carlesso, R.; Tarzia, G.; Perboni, A. EP 0502464A1; *Chem. Abstr.* **1994**, *121*, 280531.
- Selič, L. Manuscript in preparation.
- Mancuso, A. J.; Swern, D. Activated Dimethyl Sulfoxide: Useful Reagents for Synthesis. *Synthesis* **1981**, 165–185.
- (a) Afonso, A.; Hon, F.; Weinstein, J.; Gynguly, A. K. New synthesis of penems, the oxalimide cyclization reaction. *J. Am. Chem. Soc.* **1982**, *104*, 6138–6139. (b) Ernest, I.; Gosteli, J.; Woodward, R. B. The penems, a new class of β -lactam antibiotics. 3. Synthesis of optically active 2-methyl-(5R)-penem-3-carboxylic acid. *J. Am. Chem. Soc.* **1979**, *101*, 6301–6305. (c) Perrone, E.; Alpegiani, M.; Bedeschi, A.; Giudici, F.; Franceschi, G. The carbonyl-carbonyl route to penems: a stepwise analysis. *Tetrahedron Lett.* **1984**, *25*, 2399–2402. (d) Yoshida, A.; Tajima, Y.; Takeda, N.; Oida, S. An efficient carbapenem synthesis via an intramolecular Wittig reaction of new trialkoxyphosphorane-thioesters. *Tetrahedron Lett.* **1984**, *25*, 2793.
- Hanessian, S.; Desilets, D.; Bannani, Y. L. A novel ring-closure strategy for carbapenems: the total synthesis of (+)-thienamycin. *J. Org. Chem.* **1990**, *55*, 3098–3103.
- For a review see: Mitsunobu, O. The Use of Diethyl Azodicarboxylate and Triphenylphosphine in Synthesis and Transformation of Natural Products. *Synthesis* **1981**, 1–28.
- Leban, I.; Selič, L.; Mesar, T.; Čopar, A.; Solmajer, T. Precursor of a β -lactamase inhibitor: allyl (4S,8S,9R)-10-[(E)-ethylidene]-4-methoxy-11-oxo-azatricyclo[7.2.0.0^{3,8}]undec-2-ene-carboxylate. *Acta Crystallogr.* **2002**, *C58*, 367–369.
- Jeffrey, P. D.; McCombie, S. W. Homogenous, palladium(0)-catalyzed exchange deprotection of allylic esters, carbonates, and carbamates. *J. Org. Chem.* **1982**, *47*, 587.
- Herzberg, O.; Moul, J.-M. Bacterial-Resistance to Beta-Lactam Antibiotics - Crystal-Structure of Beta-Lactamase from *Staphylococcus aureus* PC1 at 2.5-Å Resolution. *Science* **1987**, *236*, 694–701.
- Dideberg, O.; Charlier, P.; Wery, J.-P.; Dehottay, P.; Dusart, J.; Erpicum, T.; Frere, J.-M.; Ghuyens, J.-M. The Crystal-Structure of the Beta-Lactamase of *Streptomyces-Albus G* at 0.3 nm Resolution. *Biochem. J.* **1987**, *245*, 911–913.
- Moews, P. C.; Knox, J. R.; Dideberg, O.; Charlier, P. Frere, J.-M. β -Lactamase of *Bacillus licheniformis* 749/C at 2 Å resolution. *Protein: Struct. Funct. Genet.* **1990**, *7*, 156–171.
- Strynadka, N. C. J.; Adachi, H.; Jensen, E. E.; Johns, K.; Sielecki, A.; Betzel, C.; Sutoh, K.; James, M. N. G. Molecular structure of the acyl-enzyme intermediate in β -lactam hydrolysis at 1.7 Å resolution. *Nature* **1992**, *359*, 700–705.
- Oefner, C.; D'Arcy, A.; Daly, J. J.; Gubernator, K.; Charnas, R. L.; Heinze, I.; Hubschwerlen, C.; Winkler, F. K. Refined crystal structure of β -lactamase from *Citrobacter freundii* indicates a mechanism for β -lactam hydrolysis. *Nature* **1990**, *343*, 284–286.

- (35) Lobkovsky, E.; Moews, P. C.; Liu, H.; Zhao, H.; Frere, J. M.; Knox, J. R. Evolution of an enzyme activity: crystallographic structure at 2 Å resolution of cephalosporinase from the ampC gene of *Enterobacter cloacae* P99 and comparison with a class A penicillinase. *Proc. Natl. Acad. Sci. U.S.A.* **1993**, *90*, 11257–11261.
- (36) Jelsch, C.; Mourey, L.; Masson, J. M.; Samama, J. P. Crystal structure of *Escherichia coli* TEM1 β -lactamase at 1.8 Å resolution. *Proteins: Struct. Funct. Genet.* **1993**, *16*, 364–383.
- (37) Maveyraud, L.; Massova, I.; Birck, C.; Miyashita, K.; Samama, J. P.; Mobashery, S. Crystal Structure of 6- α -(Hydroxymethyl)penicillanate Complexed to the TEM-1 β -Lactamase from *Escherichia coli*: Evidence on the Mechanism of Action of a Novel Inhibitor Designed by a Computer-Aided Process. *J. Am. Chem. Soc.* **1996**, *118*, 7435–7440.
- (38) Usher, K. C.; Blaszcak, L. C.; Weston, G. S.; Shoichet, B. K.; Remington, S. J. Three-dimensional structure of AmpC β -lactamase from *Escherichia coli* bound to a transition state analogue: possible implications for the oxyanion hypothesis and for inhibitor design. *Biochemistry* **1998**, *37*, 16802–16092.
- (39) Crichlow, G. V.; Nukaga, M.; Doppalapudi, V. R.; Buynak, J. D.; Knox, J. R. Inhibition of class C β -lactamases: structure of a reaction intermediate with a cephem sulfone. *Biochemistry* **2001**, *40*, 6233–6239.
- (40) Venkatesan, A. M.; Gu, Y.; Dos Santos, O.; Abe, T.; Agarwal, A.; Yang, Y.; Petersen, P. J.; Weiss, W. J.; Mansour, T. S.; Nukaga, M.; Hujer, A. M.; Bonomo, R. A.; Knox, J. R. Structure–activity relationship of 6-methylidene penems bearing tricyclic heterocycles as broad-spectrum β -lactamase inhibitors: crystallographic structures show unexpected binding of 1,4-thiazepine intermediates. *J. Med. Chem.* **2004**, *47*, 6556–6568.
- (41) Michaux, C.; Charlier, P.; Frere, J.-M.; Wouters, Crystal Structure of BRL 427215, C6-(N1-Methyl-1,2,3-triazolylmethylene)penem, in Complex with *Enterobacter cloacae* 908R β -lactamase: Evidence for a Stereoselective mechanism from Docking Studies. *J. Am. Chem. Soc.* **2005**, *127*, 3262–3263.
- (42) Chen, C. C. H.; Herzberg, O. Inhibition of Beta-Lactamase by Clavulanate-Trapped Intermediates in Cryocrystallographic Studies. *J. Mol. Biol.* **1992**, *224*, 1103–1113.
- (43) Beadle, B. M.; Trehan, I.; Focia, P. J.; Shoichet, B. K. Structural Milestones in the Reaction Pathway of an Amide Hydrolase: Substrate, Acyl, and Product Complexes of Cephalothin with AmpC Beta-Lactamase. *Structure* **2002**, *10*, 413–424.
- (44) Patera, A.; Blaszcak, L. C.; Shoichet, B. K. Crystal Structures of Substrate and Inhibitor Complexes with Ampc-Lactamase: Possible Implications for Substrate-Assisted Catalysis. *J. Am. Chem. Soc.* **2000**, *122*, 10504–10512.
- (45) Maveyraud, L.; Mourey, L.; Kotra, L. P.; Pedelacq, J.-D.; Guillet, V.; Mobashery, S. and Samama, J.-P. Structural Basis for Clinical Longevity of Carbapenem Antibiotics in the Face of Challenge by the Common Class A β -Lactamases from the Antibiotic-Resistant Bacteria. *J. Am. Chem. Soc.* **1998**, *120*, 9748–9752.
- (46) Balani, S. K.; Miwa, G. T.; Gan, L. S.; Wu, J. T.; Lee, F. W. Strategy of utilizing *in vitro* and *in vivo* ADME tools for lead optimization and drug candidate selection. *Curr. Top. Med. Chem.* **2005**, *5*, 1033–1038.
- (47) The log *P* and log *D* values for compounds **11a–h** were calculated using ACD/Labs7.0 software
- (48) Brown, A. G.; Butterworth, D.; Cole, M.; Hanscomb, G.; Hood, J. D.; Reading, C.; Rolinson, G. N. Naturally-Occurring Beta-Lactamase Inhibitors with Antibacterial Activity. *J. Antibiot.* **1976**, *29*, 668–669.
- (49) Jacobs, M. R.; Aronoff, S. C.; Joheninng, S.; Shlaes, D. M.; Yamabe, S. Comparative Activities of the Beta-Lactamase Inhibitors YTR 830, Clavulanate, and Sulbactam Combined with Ampicillin and Broad-Spectrum Penicillins against Defined Beta-Lactamase-Producing Aerobic Gram-Negative Bacilli. *Antimicrob. Agents Chemother.* **1986**, *29*, 980–985.
- (50) Sybyl program suite, Tripos Inc., St. Louis, MO, 2004.
- (51) Lobkovsky, E.; Billings, E. M.; Moews, P. C.; Rahil, J.; Pratt, R. F.; Knox, J. R. Crystallographic Structure of a Phosphonate Derivative of the *Enterobacter cloacae* P99 Cephalosporinase: Mechanistic Interpretation of a β -Lactamase Transition-State Analogue. *Biochemistry* **1994**, *33*, 6762–6772.
- (52) Merritt, E. A.; Bacon, D. J. Raster3D: Photorealistic Molecular Graphics. *Methods Enzymol.* **1997**, *277*, 505–524.
- (53) Otwinowski, Z.; Minor, W. *Methods Enzymol.* **1997**, *276*, 327–326.
- (54) Turk, D. Ph.D. Thesis, Technische Universitaet, Muenchen, 1992.
- (55) Engh, R. A.; Huber R. Accurate bond and angle parameters for X-ray protein structure refinement. *Acta Crystallogr.* **1991**, *A47*, 392–400.
- (56) Knox, J. R.; Sun, T. Refinement of P99 beta-lactamase from *Enterobacter cloacae*. 2004, PDB entry 1XX2 at www.rcsb.org.
- (57) Crichlow, G. V.; Kuzin, A. P.; Nukaga, M.; Mayama, K.; Sawai, T.; Knox, J. R. Structure of the extended-spectrum class C β -lactamase of *Enterobacter cloacae* GC1, a natural mutant with a tandem tripeptide insertion. *Biochemistry* **1999**, *38*, 10256–10261.

JM0703237